Proc. Nat. Acad. Sci. USA
Vol. 72, No. 9, pp. 3412–3415, September 1975
Biochemistry

Conformational change and cooperativity in actin filaments free of tropomyosin

(heavy meromyosin subfragment-1/magnetic resonance/spin label/manganous ion)

JOSEPH LOSCALZO, GEORGE H. REED, AND ANNEMARIE WEBER

Department of Biochemistry and Biophysics, University of Pennsylvania School of Medicine, Philadelphia, Pa. 19174

Communicated by Mildred Cohn, June 23, 1975

ABSTRACT **The decrease in amplitude of the electron spin resonance spectrum of the cysteine-bound spin-label, 3-(maleimidomethyl)-2,2,5,5-tetramethyl-1-pyrrolidinoxyl, brought about by the magnetic interaction with tightly bound manganous ion, was used as a probe of conformational change in actin on binding myosin. The magnitude of this "spin–spin" interaction first decreased then increased on increasing saturation of the actin filament with heavy meromyosin subfragment-1. That the "spin–spin" interaction occurred between spins within a single actin monomer and not between spins of adjacent monomers was demonstrated by the observation that the change in magnitude of the "spin–spin" interaction was maintained on binding of heavy meromyosin subfragment-1 to copolymers in which actin monomers containing both manganous ion and spin label were diluted 7-fold with native actin monomers. These data provide evidence for a conformational change in actin on interacting with heavy meromyosin subfragment-1. Further, the fact that not only the magnitude but also the sense of the change in the "spin–spin" interaction is a function of increasing saturation with heavy meromyosin subfragment-1 indicates that the monomers of the actin filament are capable of cooperative interaction in the absence of tropomyosin.**

Much evidence has been accumulated to show that during muscle contraction the force propelling the actin filaments toward the center of a sarcomere is generated during the interaction of myosin active sites ("myosin heads") with actin (1–4). It is likely, though not certain, that the stable intermediate, myosin·ADP·P (5, 6), forms a complex with actin which, after the release of ADP and phosphate, is transformed in such a way that the myosin heads form an acute angle with the actin filaments, producing the so-called arrowhead formation first demonstrated by Huxley (7) in actomyosin mixtures free of ATP (commonly referred to as the rigor state) and found by Reedy and his colleagues in insect flight muscle in rigor (8). In the relaxed, as well as in the rigor state, the myosin heads produce an x-ray diffraction pattern characteristic of a high degree of order, though the patterns are very different for each state (9). During contraction, however, this order is very markedly disturbed (10).

Despite the obvious gross structural differences among these different states, relatively little information has been obtained about specific protein conformational changes occurring during the various stages of actomyosin interaction. It is not known, for example, what the angle is when the myosin bridge first forms an attachment, what the specific conformational changes of the myosin molecule are, or whether any such change occurs in actin.

Direct evidence for a conformational change of actin in response to myosin binding has not even been obtained for the rigor state. We present evidence for a conformational change of actin as a result of binding of heavy meromyosin subfragment-1 in the absence of ATP, using as an indicator changes in the spin-spin interaction between Mn^{2+} bound to the unexchangeable (in the actin polymer) divalent cation site and a cysteine-bound nitroxide label. This conformational change does not seem to be restricted to the single actin monomer complexed with a myosin active site ("myosin head"), but apparently includes a response of the whole filament since the sense of change of the spin–spin interaction depends upon the extent of myosin saturation.

Abbreviations: subfragment-1, heavy meromyosin subfragment-1; G-actin, monomeric actin; F-actin, polymeric actin; SL-NEM, 3-(maleimidomethyl)-2,2,5,5-tetramethyl-1-pyrrolidinoxyl; Ca^{2+}/Mg^{2+}-actin and SL-NEM-Ca^{2+}/Mg^{2+}-actin, actin and SL-NEM-actin, respectively, containing Ca^{2+} or Mg^{2+} at each monomeric divalent cation site; Mn^{2+}-actin and SL-NEM-Mn^{2+}-actin, actin and SL-NEM-actin, respectively, containing Mn^{2+} at each monomeric divalent cation site; ESR, electron spin resonance; T_1, longitudinal relaxation time.

MATERIALS AND METHODS

Protein preparations

Heavy Meromyosin Subfragment-1 (Subfragment-1) was prepared according to Margossian and Lowey (11) with slight modifications. Myosin, precipitated by dilution, was incubated for 14 min with 15 units of papain per g of myosin in the presence of 0.2 M KCl, 5.0 mM imidazole, pH 7.0, and 0.1 mM dithiothreitol. The incubation was terminated by addition of 1.0 mM iodoacetate after lowering the pH to 6.4. Subfragment-1 was collected by ammonium sulfate precipitation between 50 and 65% saturation and dialyzed overnight against 5.0 mM imidazole, pH 7.0, and 0.2 mM dithiothreitol. These preparations routinely give a potassium-stimulated ATPase activity (in the presence of 5 mM EDTA) of 15–20 sec^{-1} and have a binding constant for actin of about 5×10^7 M^{-1} (12).

Actin was extracted in the monomeric state (G-actin) from an acetone powder of rabbit skeletal muscle prepared according to Straub (13) at 4° with 10 mM Tris buffer, pH 8.5, 0.2 mM $CaCl_2$, 0.5 mM ATP, and 0.2 mM dithiothreitol. The extract was clarified, polymerized with 0.1 M KCl and 2.0 mM $MgCl_2$, purified from the tropomyosin–troponin complex by centrifugation at 105,000 × *g* in the presence of 0.8 M KCl (14), 10 mM Tris, pH 8.5, and depolymerized again by 3-day dialysis against the extraction solution.

Actin was spin-labeled in the monomeric state in the extraction solution without dithiothreitol, using a 4-fold molar excess of 3-(maleimidomethyl)-2,2,5,5-tetramethyl-1-pyrrolidinoxyl (SL-NEM) at 4° for 2 hr. The solution was subse-

quently dialyzed extensively against extraction solution, containing dithiothreitol, to remove unbound label. Under these labeling conditions, the SL-NEM:actin stoichiometry was determined as 0.95:1.00 by denaturing the labeled actin with 5% 1 M NaOH and comparing the spectrum with those of free label standards.

Half of the SL-NEM-actin was used, after repolymerization, as the manganous ion-free control (SL-NEM-Ca^{2+}/Mg^{2+}-F-actin). The other half was converted to manganous ion-containing actin by the following treatment. First, to remove unbound calcium and magnesium, wet cation-exchange resin in the sodium form (about 10% of the actin volume) was added to the spin-labeled G-actin present at a concentration of 20 μM, in 0.1 mM ATP, 40 μM $CaCl_2$, 0.2 mM dithiothreitol, and 10 mM Tris buffer, pH 8.5 (4°). The actin was then incubated with 0.15 mM $MnCl_2$ for one hour at 4°. Polymerization with 0.1 M KCl, followed by a second cation-exchange resin treatment to remove unbound Mn^{2+} and displaced Ca^{2+} and Mg^{2+}, resulted in the formation of SL-NEM-Mn^{2+}-F-actin without free divalent cations. This F-actin was then pelleted as above. As determined by liquid scintillation counting of ^{54}Mn added as $^{54}MnCl_2$ at the incubation step (about 3.5 μCi/ml), the pelleted SL-NEM-Mn^{2+}-F-actin contained maximally 80% Mn^{2+}, more often 40–60%. That the exchange is less than 100% is presumably due to the tendency for the actin to polymerize on addition of Mn^{2+}.

Copolymers of different actin species were made by rapidly and vigorously mixing the two actin populations in the monomeric state and subsequently polymerizing with 0.1 M KCl and a small amount of F-actin, added as centers for polymerization (10% of the total final actin concentration) (15).

Determinations

Protein Concentrations were determined according to the method of Lowry *et al.* (16) after standardization of actin and myosin solutions by micro-Kjeldahl analysis, using the myosin standard curve for subfragment-1.

Inorganic Phosphate was determined according to the method of Taussky and Schorr (17).

Viscosity Measurements were performed in a water bath at 23.2°, using an Ostwald viscometer having an outflow time for water of about 60 sec, and a total volume of 10 ml.

Electron Spin Resonance (ESR) Spectra were recorded at 9.1 GHz (X-band) with a Varian E-3 spectrometer. The longitudinal relaxation time of water protons (T_1) was measured by the pulsed nuclear magnetic resonance procedure of Carr and Purcell (18) at 15.0, 24.3, and 40.0 MHz. The temperature for both ESR and proton relaxation rate measurements was regulated with a Varian model V-4340 variable temperature accessory.

The Off-Rate of Mn^{2+} from G-Actin was estimated by incubating 20 μM ^{54}Mn-containing Mn^{2+}-G-actin (treated with about 10% of its volume of wet mixed-bed ion-exchange resin to remove free Mn^{2+} and ATP) with a 20-fold excess of Ca^{2+} (as $CaCl_2$) for increasing periods of time. After each incubation, free Mn^{2+} (and ^{54}Mn) was removed by rapid mixing with about 10% of its volume of wet mixed-bed ion-exchange resin and centrifugation to pellet the resin. Since the Mn^{2+} remaining in the supernatant was all bound, i.e., less than 1 μM free (as determined by the disappearance of the spectrum of free Mn^{2+} by ESR), the amount of Mn^{2+} released was given by the difference of actin-bound ^{54}Mn before and after incubation with Ca^{2+}.

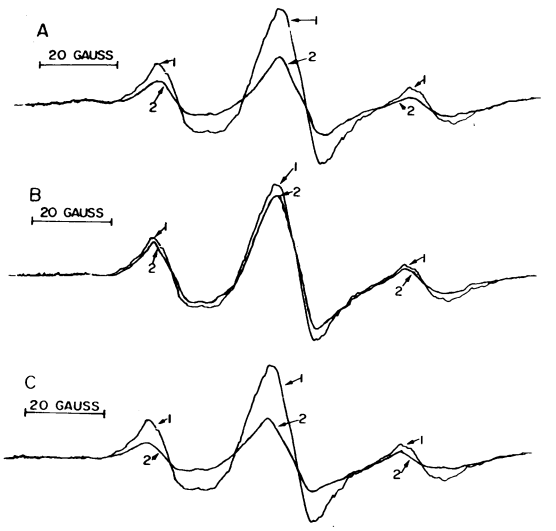

FIG. 1. ESR spectra of SL-NEM showing the influence of binding of subfragment-1 to actin filaments on the spin–spin interaction between Mn^{2+} and SL-NEM. All samples contained 38 μM F-actin in 10 mM Tris buffer, pH 8.0, 0.1 M KCl, and 0.2 dithiothreitol. 60% Mn^{2+} was incorporated in the SL-NEM-Mn^{2+}-F-actin. A, B, and C refer to 0, 30, and 100% F-actin saturation with subfragment-1, respectively. 1 and 2 identify spectra of SL-NEM-Ca^{2+}/Mg^{2+}-F-actin and SL-NEM-Mn^{2+}-F-actin, respectively, at each level of saturation. Spectra were recorded at 23° with a modulation amplitude of 2.5 G and 50 mW microwave power.

RESULTS

The spin–spin interaction between SL-NEM and Mn^{2+} bound to G-actin persisted after the actin polymerization, as observed previously by Burley and his colleagues (19). Fig. 1A shows that the SL-NEM ESR signal amplitude was quenched in the presence of Mn^{2+} relative to that of Mn^{2+}-free F-actin. Addition of subfragment-1 to 30% saturation increased the signal amplitude substantially (Fig. 1B). At complete saturation, the signal amplitude decreased again, returning to a value lower than that observed before subfragment-1 addition (Fig. 1C). Fig. 2 indicates this biphasic

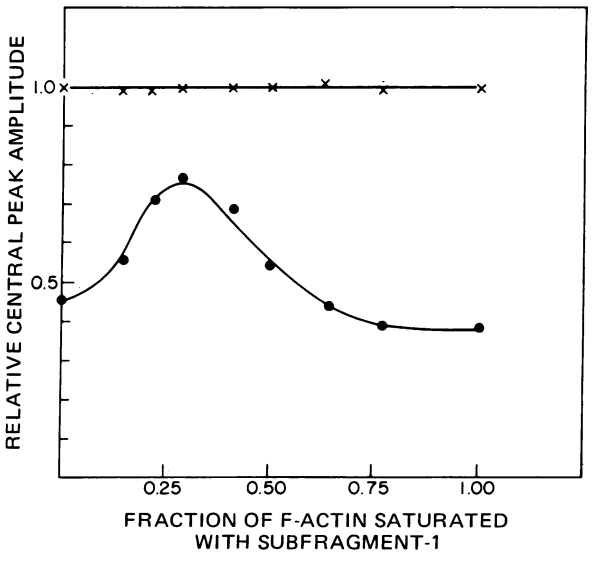

FIG. 2. Relative central peak amplitude of SL-NEM ESR spectra as a function of F-actin saturation with subfragment-1 for SL-NEM-Ca^{2+}/Mg^{2+}-F-actin (×) and SL-NEM-Mn^{2+}-F-actin (●). Same experiment as in Fig. 1.

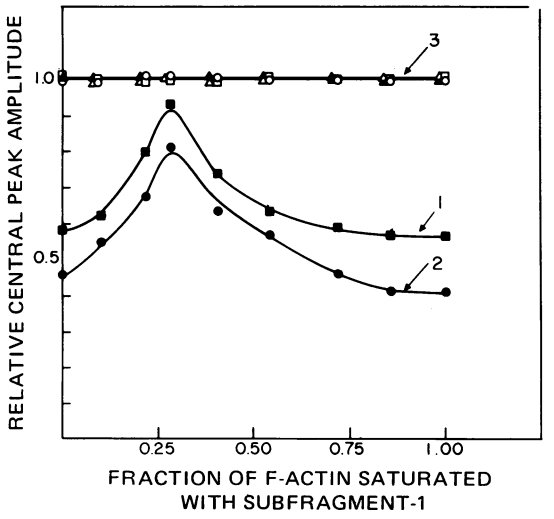

FIG. 3. The response (relative central peak amplitude) of randomly mixed copolymers to increasing saturation with subfragment-1. Curve 1: (■) copolymer containing 14% doubly labeled actin (60% Mn^{2+} substitution) and 86% control (unmodified) actin at 7.0 relative gain to correct for the concentration difference of SL-NEM-Mn^{2+}-actin between curves 1 and 2. Curve 2: (●) pure SL-NEM-Mn^{2+}-F-actin used for the copolymer of curve 1, 1.0 relative gain. Curve 3: Mn^{2+}-free controls for curves 1 (□) and 2 (○) at relative gains of 7.0 and 1.0, respectively; copolymer of an equimolar mixture of Mn^{2+}-actin and SL-NEM-Ca^{2+}/Mg^{2+}-actin (▲) and the control curve with Mn^{2+}-free actin (△) at a relative gain of 2.0 to correct for the reduction in the SL-NEM concentration.

change in the central peak height of the SL-NEM ESR spectrum of SL-NEM-Mn^{2+}-F-actin relative to that of SL-NEM-Ca^{2+}/Mg^{2+}-F-actin on increasing filament saturation with subfragment-1.

The changes in peak amplitude are not due to changes in correlation time for spin–spin interaction. The dominant correlation time for the spin–spin interaction is probably the electron spin relaxation time of Mn^{2+} (20). The correlation time for the interaction of Mn^{2+} with water protons is also dominated by the electron spin relaxation time. The frequency dependence of water proton relaxation rates shows that there is virtually no change in the correlation time on addition of subfragment-1 in increasing concentrations (Table 1). In addition, the ESR spectrum for the SL-NEM indicated that subfragment-1 binding did not result in an observable change in the rotational freedom of the label (Fig. 1).

The effect of the unpaired spin of Mn^{2+} on the ESR spectrum of the SL-NEM is governed by the separation of the two spins and a "structural" angle (20). The fact that the amplitudes of all three peaks in the SL-NEM spectrum were influenced by the same relative amounts at each level of subfragment-1 saturation suggests that subfragment-1 binding changes the extent of the spin–spin interaction primarily by altering the distance between the two spins (Fig. 1).

From the experiment of Fig. 2, one cannot ascertain whether the Mn^{2+} and SL-NEM on the same or on two neighboring actin monomers interact. If the magnetic interaction occurs between spins on adjacent monomers, changes in peak height would not be observed if each SL-NEM-Mn^{2+}-actin molecule were surrounded by Ca^{2+}/Mg^{2+}-actin monomers in the filament. However, the change in peak height would persist in actin filaments consisting of a mixture of Mn^{2+}-actin and SL-NEM-Ca^{2+}/Mg^{2+}-actin molecules. The preparation of actin filaments consisting of two randomly mixed populations of actin monomers was possible because the loss of Mn^{2+} from the divalent cation site of G-actin has a half-time of >24 sec (see *Materials and Methods*). This provides ample time for mixing and polymerizing the two populations of actin monomers before appreciable exchange of Mn^{2+} occurs.

Table 1. Mn^{2+}-water proton correlation time (τ_c) for Mn^{2+}-F-actin with increasing subfragment-1 saturation.

Saturation (%)	$\tau_c \times 10^9$ (sec)
0	5.1
30	5.0
100	4.9

τ_c was determined according to the method of Peacocke *et al.* (21) from plots of the difference of $1/T_1$ for Mn^{2+}-F-actin and $1/T_{1_s}$ for Mn^{2+}-free F-actin against $(2\pi f)^2$ for each level of saturation with subfragment-1.

Fig. 3 shows that the changes in the amplitude of the ESR signal were maintained when SL-NEM-Mn^{2+}-actin was diluted 7-fold by copolymerization with Ca^{2+}/Mg^{2+}-actin and lost when filaments consisted of an equal amount of Mn^{2+}-actin and SL-NEM-Ca^{2+}/Mg^{2+}-actin.

These observations indicate that Mn^{2+} and SL-NEM of the same monomer interact, provided that truly random copolymers form and the two species of actin do not segregate to form two sets of homogeneous polymers. That the perturbation created by the presence of Mn^{2+} or SL-NEM in an actin monomer does not affect the process of polymerization is suggested by the observation that the rate of polymerization, as measured by viscosity increase as well as inorganic phosphate release, was not significantly different from that of unlabeled actin. Both phosphate release [due to hydrolysis of ATP bound to the actin monomer (22)] and specific viscosity changes follow exactly the same time course (Fig. 4). Fig. 4 shows identical polymerization rates for Ca^{2+}/Mg^{2+}-actin, SL-NEM-Ca^{2+}/Mg^{2+}-actin, Mn^{2+}-actin, and SL-NEM-Mn^{2+}-actin.

DISCUSSION

A spin–spin interaction between tightly bound Mn^{2+} and a maleimide spin label was first demonstrated by Burley and his colleagues (19) and later confirmed by Burley and Sleigh (23). Assuming the maleimide spin label binds exclusively to a single cysteine [as suggested by previous reports on cysteine labeling of actin (24)], an extrapolation to 100% Mn^{2+} incorporation gives about 85% maximal reduction in the height of the central peak of the SL-NEM ESR signal in the absence of subfragment-1, and clearly indicates the proximity of the Mn^{2+} and the SL-NEM.

Since a reduction in peak height was observed under conditions where actin is usually present in the monomeric state (19), it was considered likely that in the actin polymer the Mn^{2+} and the SL-NEM of the same monomer interact. However, in view of the significance of the change in the spin–spin interaction on subfragment-1 binding, it seemed important to check whether this remained entirely an intrasubunit interaction after actin polymerization. The data with randomly mixed copolymers, which show a change in the spin–spin interaction when doubly labeled actin monomers are surrounded by unlabeled molecules and no spin–spin interaction between the two spins on neighboring actin molecules, indicate that the spin–spin interaction is, indeed, entirely intrasubunit, provided that the copolymerization is

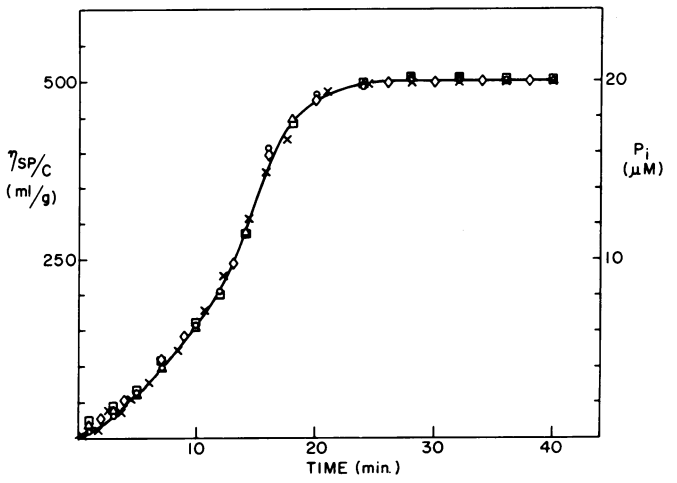

FIG. 4. Viscosity increase and inorganic phosphate release as a function of time of polymerization of actins containing different kinds of labels. The polymerization of control Ca^{2+}/Mg^{2+}-actin was followed by viscosity increase (×) as well as inorganic phosphate release (○), while the polymerization of Mn^{2+}-actin (△), SL-NEM-Ca^{2+}/Mg^{2+}-actin (□), and SL-NEM-Mn^{2+}-actin (◇) were all followed by viscosity increase. All actins were prepared from the same stock solution, and all final concentrations were 22 μM in 10 mM Tris buffer, pH 8.0, 0.1 M KCl, 0.2 mM dithiothreitol, and 0.1 mM ATP.

truly random. The latter, although not certain, is likely because the kinetics of actin polymerization were not altered by the presence of either of the labels.

The above data, coupled with the observations that there is no appreciable change in either the correlation time for the interaction between Mn^{2+} and SL-NEM (as approximated by that between Mn^{2+} and water protons) or the line shape of the SL-NEM bound to F-actin on subfragment-1 binding, indicate a conformational change in actin on subfragment-1 binding. This change seems to involve a change in the distance between manganous ion and the nitroxide label rather than a change in structural angle (20) since parallel and perpendicular components of the SL-NEM spectrum were influenced to the same extent on subfragment-1 binding (Fig. 1). It is too early for any quantitative statements concerning the extent of the conformational change. That must await 100% Mn^{2+} incorporation and analysis of the SL-NEM-containing actin peptide for homogeneity.

However, the biphasic nature of the response suggests cooperativity of some kind, since binding of subfragment-1 molecules elicited quite different responses at different degrees of saturation of the actin filament with subfragment-1. This biphasic behavior of the spin–spin interaction on increasing saturation with subfragment-1 is very similar to the biphasic change in ultraviolet absorption and elastic light scattering on increasing saturation with heavy meromyosin observed by Tawada (25) and Fujime and Ishiwata (26), respectively.

These ESR studies establish that the biphasic response originates from conformational changes within the actin molecules in the filament. They also provide evidence that not all of the cooperative behavior within the actin filament is dependent on tropomyosin. Tropomyosin simply adds additional protein–protein interactions to a filament already capable of cooperative interactions among monomers. Furthermore, the observation that conformational changes in actin molecules can be cooperative should make one hesitant to ascribe all cooperative phenomena in the presence of tropomyosin to positional changes of tropomyosin. In this respect, it is interesting that Yanagida and his collaborators (27) interpret their linear dichroism data to mean that in regulated filaments calcium causes conformational changes in actin.

J.L. is supported by an M.S.T.P. award from the National Institutes of Health (GM 02046-05-S1). This investigation was supported by National Institute of Arthritis, Metabolic and Digestive Diseases Research Career Development Award no. 5-K04-AM 70134, National Institutes of Health Research Grant no. AM 17517 to G.H.R., and National Institutes of Health Research Grant no. HL 15835-02 to A.W.

1. Weber, A. & Murray, J. M. (1973) *Physiol. Rev.* **53**, 612–673.
2. Taylor, E. W. (1972) *Annu. Rev. Biochem.* **41**, 577–616.
3. Huxley, H. E. (1969) *Science* **164**, 1356–1366.
4. Huxley, A. F. (1974) *J. Physiol.* **243**, 1–43.
5. Lymn, R. W. & Taylor, E. W. (1970) *Biochemistry* **9**, 2975–2983.
6. Trentham, D. R., Bardsley, R. G., Eccleston, J. F. & Weeds, A. G. (1972) *Biochem. J.* **126**, 635–644.
7. Huxley, H. E. (1963) *J. Mol. Biol.* **7**, 281–308.
8. Reedy, M. K., Holmes, K. C. & Tregear, R. T. (1965) *Nature* **207**, 1276–1280.
9. Huxley, H. E. (1968) *J. Mol. Biol.* **37**, 507–520.
10. Huxley, H. E. & Brown, W. (1967) *J. Mol. Biol.* **30**, 383–434.
11. Margossian, S. S. & Lowey, S. (1973) *J. Mol. Biol.* **74**, 301–312.
12. Marston, S. & Weber, A. (1975) *Biochemistry*, in press.
13. Straub, F. B. (1942) *Stud. Inst. Med. Chem. Univ. Szeged.* **2**, 3–22.
14. Spudich, J. A. & Watts, S. (1971) *J. Biol. Chem.* **246**, 4866–4871.
15. Asakura, S., Taniguchi, M. & Oosawa, F. (1963) *J. Mol. Biol.* **7**, 55–69.
16. Lowry, O. H., Rosebrough, N. J., Farr, A. L. & Randall, R. J. (1951) *J. Biol. Chem.* **193**, 265–275.
17. Taussky, H. H. & Schorr, E. (1953) *J. Biol. Chem.* **202**, 675–685.
18. Carr, H. Y. & Purcell, E. M. (1954) *Phys. Rev.* **94**, 630–638.
19. Burley, R. W., Seidel, J. C. & Gergely, J. (1969) *Arch. Biochem. Biophys.* **150**, 792–796.
20. Leigh, J. S., Jr. (1970) *J. Chem. Phys.* **52**, 2608–2612.
21. Peacocke, A., Richards, R. E. & Sheard, B. (1969) *Mol. Phys.* **16**, 177–189.
22. Straub, F. V. & Feuer, G. (1950) *Biochim. Biophys. Acta* **4**, 455–470.
23. Burley, R. W. & Sleigh, R. W. (1973) *Arch. Biochem. Biophys.* **159**, 792–801.
24. Martonosi, A. (1968) *Arch. Biochem. Biophys.* **123**, 29–40.
25. Tawada, K. (1969) *Biochim. Biophys. Acta* **172**, 311–318.
26. Fujime, S. & Ishiwata, S. (1971) *J. Mol. Biol.* **62**, 251–265.
27. Yanagida, T., Taniguichi, M. & Oosawa, F. (1974) *J. Mol. Biol.* **90**, 509–522.